Soft Matter

Cite this: *Soft Matter*, 2011, **7**, 6213

www.rsc.org/softmatter

PAPER

Supramolecular organogels based on perylenetetracarboxylic diimide dimer or hexamer†

Lin Xue,[a] Haixia Wu,[a] Yan Shi,[a] Heyuan Liu,[a] Yanli Chen*[b] and Xiyou Li*[a]

Received 11th March 2011, Accepted 13th April 2011
DOI: 10.1039/c1sm05435j

Two new perylenetetracarboxylic diimide (PDI) derivatives, namely dimer **1** and hexamer **2** composed of two or six PDI units respectively, are prepared. The aggregation behaviour of these two compounds in solution was investigated using absorption and fluorescence spectra. The results indicate that hexamer **2** tries to form large molecular aggregates *via* an intermolecular process even in very dilute solution. But dimer **1** prefers to take a folded conformation with the two PDI units stacking in a face-to-face way *via* an intramolecular process. Infrared spectra revealed the presence of hydrogen bonding between the amide nitrogen and carbonyl oxygen in the molecular aggregates of dimer **1** and hexamer **2**. The morphology of the dried gel of dimer **1** shows bundles of long fibres with very large aspect ratios. But hexamer **2** presents only small rod-like aggregates with small aspect ratio. This difference is likely caused by the competition between different driving forces for the molecular aggregation.

Introduction

In recent years, low molecular weight organic gelators have attracted widespread research interest due to their numerous potential industrial applications as well as their interesting supramolecular architectures.[1–3] This research aimed at not only understanding the fundamental aggregate structures in the gels at different scales, but also explored their potential for futuristic technological applications. For example: gels have been used as sensors,[4] as templates to prepare novel inorganic superstructures,[5] and as light harvesting arrays.[6–8]

Perylenetetracarboxylic diimides (PDI) are currently being investigated for use in a variety of photoactive organic materials.[9] They are excellent building blocks for self-organized molecular materials due to the strong π–π interactions between the planar PDI rings.[10,11] Recently, different functional groups have been introduced at the imide nitrogen atoms or the bay positions of PDI with the aim of modifying the micro structures as well as the morphology of the molecular aggregates. Organogels based on the self-assembly of PDI molecules through different weak interactions, have successfully been used as photonic[12] and electronic materials.[13] Shinkai and co-workers have prepared a series of PDI compounds by connecting cholesterol groups at the imide nitrogen position, which can form organic gel with light harvesting functions.[14] Würthner and co-workers have reported a highly fluorescent organic gel based on a PDI compound functionalized with urea groups.[15] Rybtchinski *et al.* have recently prepared an amphiphilc PDI compound by connecting a long hydrophilic chain at the bay positions. This compound can form linear molecular aggregates and shows different response towards multiple outer stimuli.[16]

We and other research groups have demonstrated successfully that connecting several plannar aromatic rings in one molecule is an efficient way to enforce the interactions between two molecules and thus leads to the formation of molecular aggregates with long range order.[17–19] With this in mind, we designed two new PDI molecules, dimer **1** and hexamer **2** as shown in Scheme 1, which contain two or six PDI units in one molecule respectively. Moreover, long alkyl chains are introduced at one end of these molecules, which are expected also to promote the molecular aggregation in solution as revealed in literature.[20] We believe that strong interactions between these molecules could be achieved and thus long range order in their molecular aggregates can be established.

Results and discussion

Molecular design and synthesis

PDIs with no substituent at the bay positions have very strong π–π interactions and therefore are ideal building blocks for the construction of ordered molecular aggregates.[21] But their low solubility in conventional organic solvents has seriously limited further modification of their molecular structure. In contrast, 1,7-diphenoxyl substituted PDIs have not only strong π–π

[a]*Key lab of Colloid and Interface Chemistry, Ministry of Education, Department of Chemistry, Shandong University, China 250100. E-mail: xiyouli @sdu.edu.cn; Fax: +86 (0)531 8836 9877*
[b]*Department of Chemistry, University of Jinan, Jinan, 250100, PR China*

† Electronic supplementary information (ESI) available: The fluorescence spectra and fluorescence quantum yields of hexamer **2** in $CHCl_3$ at different concentrations, temperature-dependent absorption spectra of dimer **1** in MCH, and the fluorescence spectrum of dimer **1** in MCH (5×10^{-8} mol L^{-1}). See DOI: 10.1039/c1sm05435j

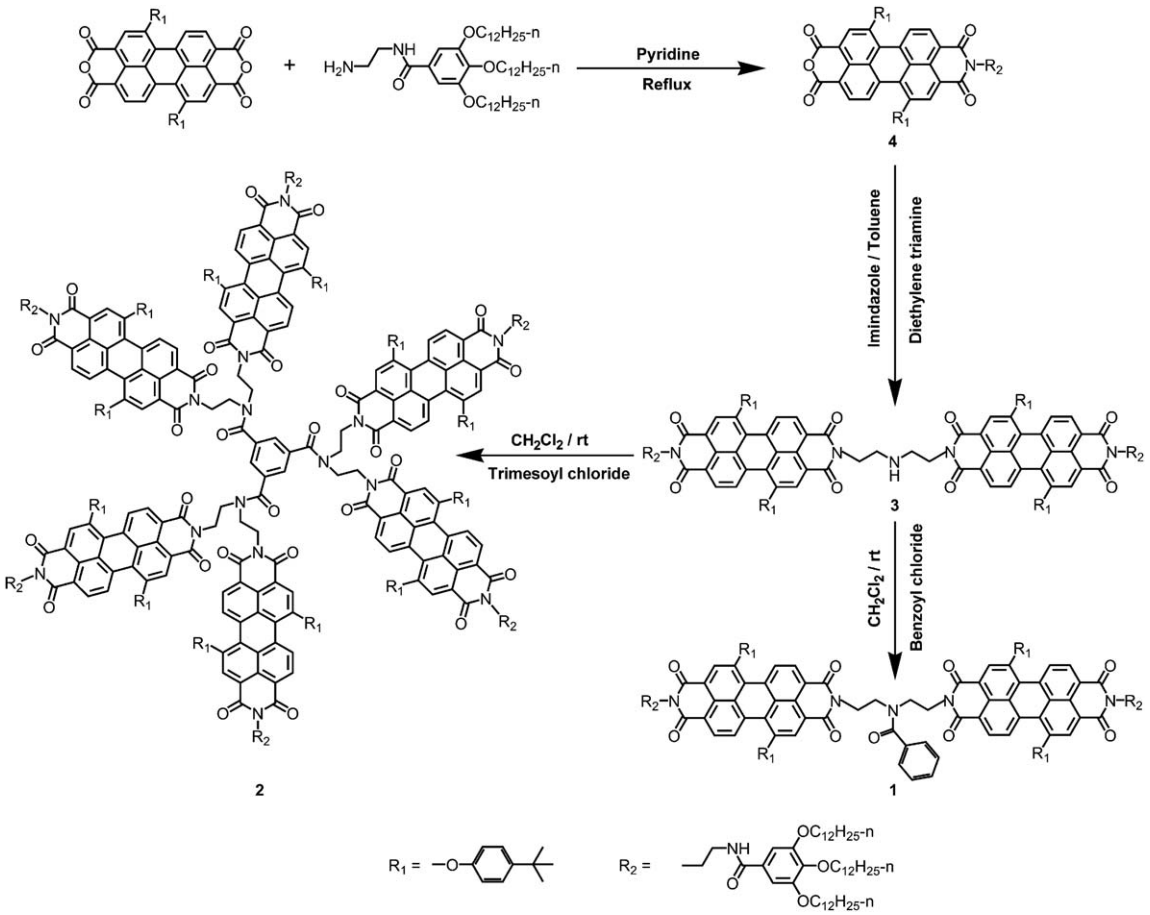

Scheme 1 Synthesis of dimer **1** and hexamer **2**.

interactions between their molecules, but also reasonable solubility in conventional organic solvents. The synthetic and purification procedures of 1,7-diphenoxyl substituted PDIs are therefore much easier than those of non-substituted PDIs. The compounds we designed in this work need several steps to modify the molecular structure. In order to avoid difficulties in the synthesis and purification, we chose 1,7-diphenoxyl substituted PDIs as the building blocks for the dimer and hexamer.

The synthetic procedures used for the dimer and hexamer are shown in Scheme 1. 1,7-Di(*p*-*t*-butyl-phenoxyl)-3,4,9,10- tetracarboxylic dianhydride reacts first with *N*-(2-aminoethyl)-3,4,5-tris(dodecyloxy)benzamide[12] in refluxing pyridine to give the important intermediate **4**. Compound **4** reacts further with diethylene triamine in a mixed solvent of imidazole/toluene to give compound **3** with reasonable yield. The benzoylation of compound **3** with benzoyl chloride or trimesoyl chloride gives dimer **1** or hexamer **2** respectively. All the new compounds were fully characterized with ^{1}H NMR, MALDI-TOF mass spectra, as well as elemental analysis.

UV-vis absorption and fluorescence spectra in chloroform

UV-vis absorption and fluorescence spectra of PDIs are sensitive to the interchromophore distance and orientation,[22,23] and therefore, have been widely used to study their π–π stacking.[24–26] Fig. 1 shows the absorption and emission spectra of dimer **1** and hexamer **2** in diluted $CHCl_3$ solution.

The absorption spectra of dimer **1** in $CHCl_3$ (10^{-7} mol L^{-1}) resemble that of a monomeric PDI in solution (Fig. 1a).[27] The absorption maxima at 552 nm was attributed to the 0–0 transition, whereas the small shoulder at about 515 nm can be assigned to the 0–1 transition. The emission spectrum with a band maximum at 590 nm is the mirror image of the absorption band and copies the characteristics of the PDI monomer's fluorescence spectrum. This result suggests that the two PDI units in dimer **1** do not show any interactions in diluted solution. However, the absorption spectrum of hexamer **2** as shown in Fig. 1b is significantly different from that of monomeric PDI. The relative intensity of the maximum absorption band at about 555 nm against that of the band at 515 nm decreased significantly. This change in the absorption spectrum suggests that there is strong interaction between the PDI units of hexamer **2** due to formation of H aggregates. The fluorescence spectra of hexamer **2** reveal a similar emission band at about 588 nm to that of monomeric PDI or dimer **1**. But the fluorescence quantum yield decrease dramatically (from 98% for the monomeric PDI to 4.67% for the haxamer **2**). The drop on the fluorescence quantum yield is also strong evidence for the formation of molecular aggregates of PDI,[19] which is in line with the results from the absorption spectra.

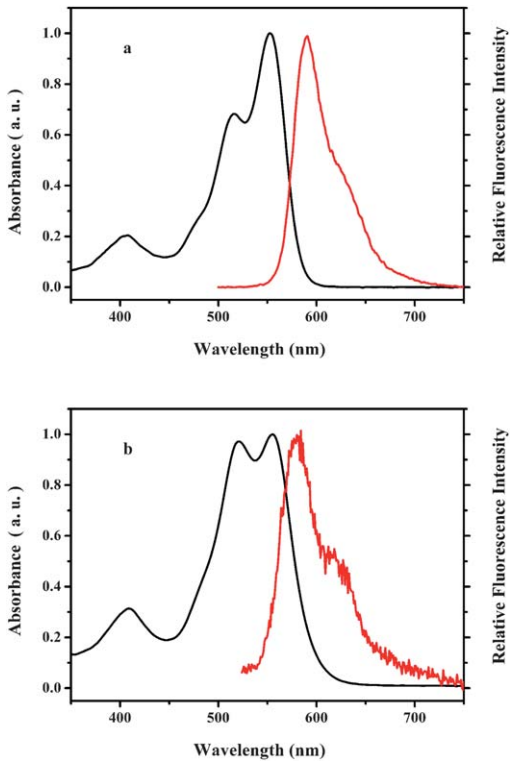

Fig. 1 Normalized absorption (black) and emission (red) spectra of dimer **1** (a) and hexamer **2** (b) in diluted $CHCl_3$.

Now a critical question arising from this result is are the aggregates of PDIs in hexamer **2** are formed *via* an intermolecular or intramolecular process? As mentioned above, both fluorescence and absorption spectra are recorded in a solution of chloroform with a concentration of 10^{-7} mol L^{-1}. Normally, no intermolecular interaction can be observed in such a dilute solution. However, the absence of aggregation for the PDIs in dimer **1** as revealed by the absorption spectra seems to support an intermolecular process. Moreover, due to the presence of multiple long alkyl chains and PDI rings, the intermolecular interaction between hexamer **2** units is expected to be much stronger, and it is possible that hexamer **2** forms dimeric or even larger molecular aggregates in dilute solution.[18] To verify our hypothesis, the absorption and fluorescence spectra of hexamer **2** in chloroform at different concentrations were recorded. It was found that, the absorption spectra of hexamer **2** are not affected significantly by the concentration, but the fluorescence spectra as well as the fluorescence quantum yields are significantly affected by the concentration in the range of 10^{-7}–10^{-5} mol L^{-1}, Fig. S1 (ESI†). As reported previously, fluorescence spectroscopy is more sensitive to molecular aggregation than absorption spectroscopy.[28] The drop on the fluorescence quantum yields along with the concentration increase can be ascribed to the formation of molecular aggregates. This result suggests that the aggregation of PDI in hexamer **2** is concentration dependent and supports the hypothesis of intermolecular aggregation.

The aggregation behavior in diluted MCH solution

The long alkyl chains in dimer **1** and hexamer **2** are well known for their abilities to induce the formation of highly ordered molecular aggregates in non-polar organic solvents.[13] The absorption spectra of dimer **1** in non-polar solvent methyl cyclohexane (MCH) at low concentrations (10^{-7} M) are shown in Fig. 2a. Compared to that in chloroform, the absorption peak intensity at 555 nm is almost equal to that at 515 nm. These changes in the absorption spectra suggest the presence of aggregation of the PDI units in MCH. In order to identify whether the aggregation of PDI is an intermolecular or an intramolecular process, the concentration dependent absorption spectra of dimer **1** in MCH in a concentration range of 1×10^{-7}–5×10^{-5} mol L^{-1} were recorded, but no distinctive change to the absorption spectra with concentration change can be observed. This result indicates that the aggregation of dimer **1** in MCH is concentration independent. The fluorescence spectra of dimer **1** in MCH show a broad emission band in the range of 550–800 nm, Fig. 2a. It is completely different from that in chloroform as shown in Fig. 1a and can be assigned to the emission of an "excimer-like" state due to the formation of face-to-face stacked PDI dimers.[28,29] This is in line with the results deduced from the absorption spectra. It is interesting that the emission bands in the fluorescence spectra do not change in shape with concentration increase (tested concentration range 5×10^{-8}–5×10^{-5} mol L^{-1} Fig. S3(ESI†)). Moreover, the fluorescence quantum yields as shown in Fig. 2b are almost constant in the concentration rang of 10^{-8}-10^{-5} mol L^{-1}. This result suggests that the aggregates of PDI of dimer **1** in MCH are concentration independent.

The weak intermolecular interactions between the adjacent molecules in a supramolecular system are easily broken by a rise

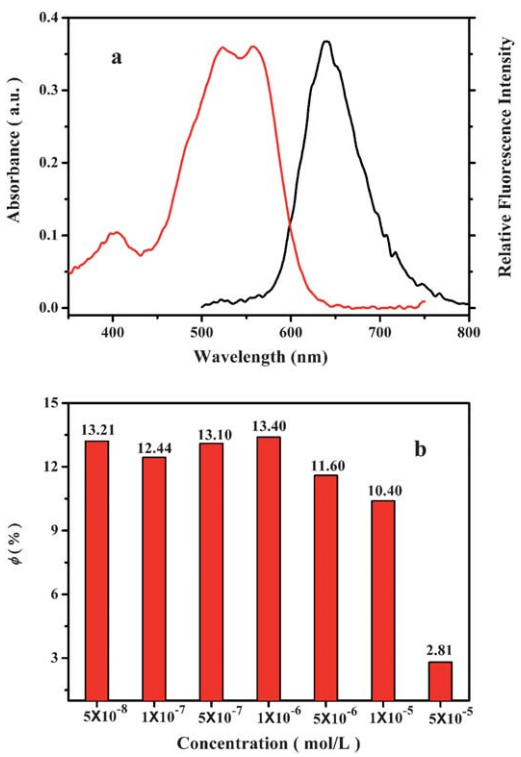

Fig. 2 The normalized absorption and fluorescence spectra (a) of dimer **1** in diluted MCH and its fluorescence quantum yields at different concentrations (b).

in temperature. Therefore the temperature dependent absorption and emission spectra are also an efficient way of identifying intra- and inter-molecular processes of the aggregation. The temperature dependent absorption spectra of dimer **1** in MCH revealed no changes along with temperature increase, Fig. S2(ESI†). The temperature dependent fluorescence spectra of dimer **1** in MCH do not present a significant change in shape with temperature increase, but a remarkable decrease in the fluorescence quantum yields. This fluorescence quantum yield decrease suggests that the aggregation of PDIs in dimer **1** has been enforced due to the temperature increase. These results support the hypothesis that the aggregation of dimer **1** in MCH can not be broken by a rise in temperature and is an intramolecular aggregation process, *i.e.* folding of a molecule of dimer **1**.

The absorption spectra of hexamer **2** in MCH (10^{-7} M) are different from that in chloroform (Fig. 3a). The absorption peak show a distinctive intensity reverse between the absorption band at 555 and 515 nm, which indicates the formation of face-to-face stacked aggregates of hexamer **2** in MCH. The absorption spectra of hexamer **2** in MCH at different concentrations present no further change and suggest that the absorption spectra are concentration independent. However, the fluorescence spectra of hexamer **2** in MCH are change significantly along with concentration increase as shown in Fig. 3b. When the concentration is extremely small, such as 10^{-7} mol L^{-1}, hexamer **2** presents a fluorescence spectrum with the maximum emission peak at about 668 nm. This result reveals significant aggregation for the PDI units of hexamer **2** in MCH at this concentration, which is in accordance with the results from the absorption spectra.

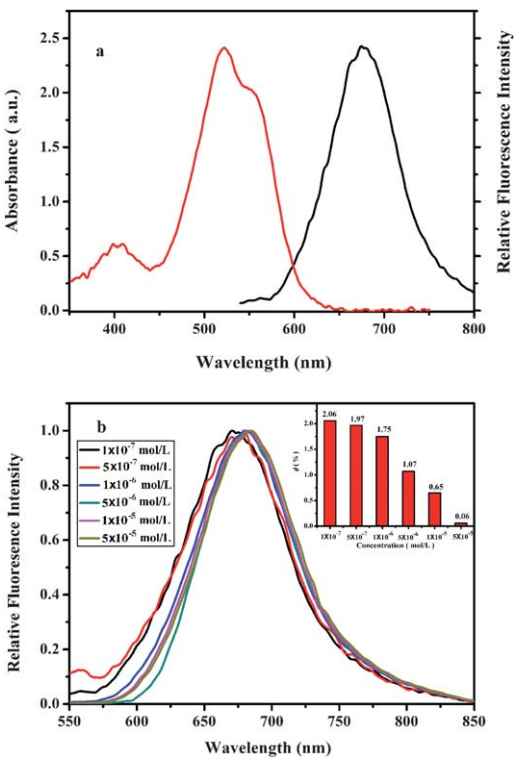

Fig. 3 Normalized absorption and fluorescence spectra (a) of hexamer **2** in diluted MCH, normalized fluorescence spectra of hexamer **2** (b) and corresponding fluorescence quantum yields (inset) at different concentrations in MCH.

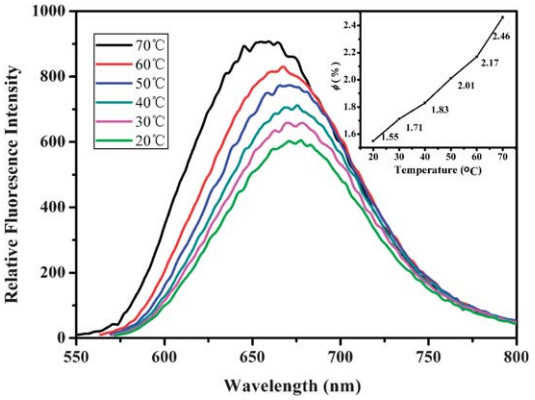

Fig. 4 The fluorescence spectra and fluorescence quantum yields (inset) of hexamer **2** in MCH (5×10^{-6} mol L^{-1}) at different temperatures.

However, when the concentration of hexmaer **2** in MCH increases from 10^{-7} to 10^{-6} mol L^{-1}, the maximum emission band red-shifts significantly from 668 to 680 nm, which can be assigned to the "excimer-like" states and indicates the enhancement of the face-to-face stacked structure for the PDI aggregates due to the concentration increase. This result suggests that the aggregation of PDI units of hexamer **2** in MCH is enhanced as the concentration increases. This result indicates that the aggregation of hexamer **2** in MCH was caused at least partially by the intermolecular process. The temperature dependent absorption spectra of hexamer **2** in MCH reveals again no changes with rising temperature, it seems that the aggregates of hexamer **2** can not be broken by an increase in temperature. The fluorescence spectra of hexamer **2** in MCH do not change obviously in shape as well as maximum emission wavelength along with temperature increase, but a significant increase of fluorescence quantum yield is observed, Fig. 4. The remarkable increase of the fluorescence quantum yield is ascribed to the dissociation of the molecular aggregates of hexamer **2** at high temperature. Based on the temperature dependent absorption and fluorescence spectra of hexamer **2**, one can divide the aggregation of hexamer **2** in MCH into two steps, in the first step the PDI units in hexamer **2** aggregate in a face-to-face stacked way *via* an intramolecular process, this is why we can observe significant aggregation of PDIs at very low concentration. In the second step, the molecules of hexamer **2** driven by the hydrophobic interactions between the long alkyl chains self-assemble into large molecular aggregates *via* an intermolecular process. The face-to-face stacked structure for the PDI units is reinforced by the intermolecular aggregation. The second step of the aggregation can be disrupted by low concentration as well as high temperature.

Hydrogen bonding

Besides the strong π–π interaction, we expect that hydrogen bonding between the amide hydrogen atom and the carbonyl oxygen atom is another driving force for the aggregation of the PDI units in dimer **1** and hexamer **2**. To verify this speculation, the IR spectra of dimer **1** and hexamer **2** in chloroform and MCH were recorded, Fig. 5. The IR spectra of these two compounds in $CHCl_3$ all show a broad N–H stretching band at about 3400 cm^{-1}, which indicates the absence of hydrogen bonding.[30] But in MCH solution, the N–H stretching band emerges at

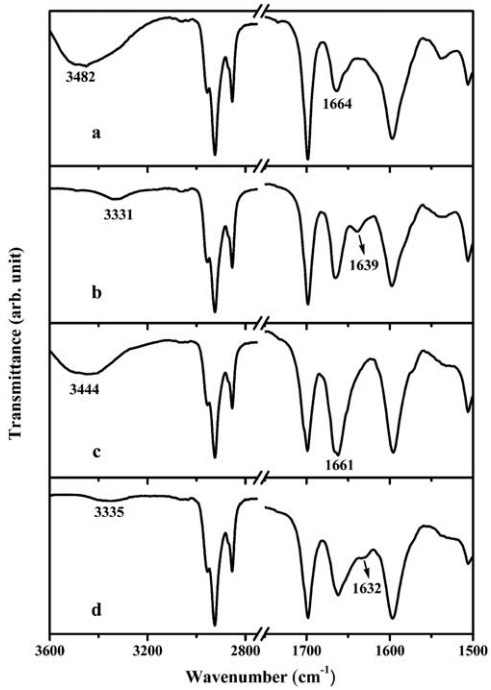

Fig. 5 IR spectra of dimer **1** in $CHCl_3$ solution (a, 1.0×10^{-3} mol L^{-1}) and in MCH solution (b, 1.0×10^{-3} mol L^{-1}), and IR spectra of hexamer **2** in $CHCl_3$ solution (c, 1.0×10^{-3} mol L^{-1}) and in MCH solution (d, 1.0×10^{-3} mol L^{-1}).

a lower frequency of about 3300 cm^{-1}. Meanwhile, the benzamide carbonyl group vibration band which overlaps with the carbonyl group vibration of imide group at 1660 cm^{-1} in $CHCl_3$ shift to 1630 cm^{-1} in MCH. Both displacements to a lower frequency are indicative of hydrogen-bonding interactions among the amide moieties.[30]

Gelating properties

Due to the good aggregation properties revealed by the spectroscopic properties as mentioned above, we expect good gelating properties for both dimer **1** and hexamer **2**. The gelating abilities were then tested in several organic solvents. The compounds and the solvent were put together in a glass sample vial and it was heated until everything was dissolved then cooled down to room temperature. After leaving the sample for two days at ambient temperature, we invert the vial to check the state of the solution. Both dimer **1** and hexamer **2** are found to form gel in MCH but do not in polar solvents, such as acetone, dioxane and THF. The critical gelation concentrations of dimer **1** and hexamer **2** in MCH are determined to be 3.4 mmol L^{-1} and 1.1 mmol L^{-1} respectively at room temperature, Fig. 6.[31]

The absorption and fluorescence spectra of the gel of dimer **1** and hexamer **2** are shown in Fig. 7. The absorption spectra of the gel of dimer **1** show similar absorption spectra to that in diluted MCH solution except for the distinctive broadening of the absorption peaks. The fluorescence spectra of the gel of dimer **1** present a further red-shift on the maximum emission peak (658 nm) relative to that in MCH solution (640 nm), which can be attributed to the further intermolecular aggregation of dimer **1** in the gel state.

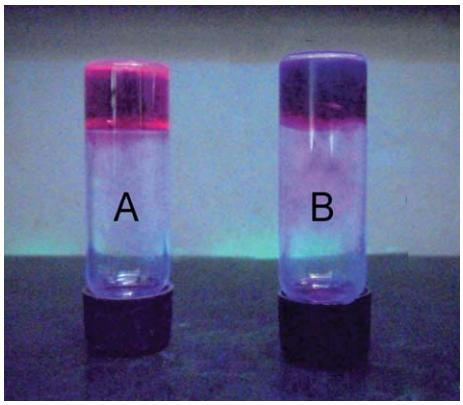

Fig. 6 Photographs of dimer **1** (A) and hexamer **2** (B) in MCH solvent under a UV light (365 nm).

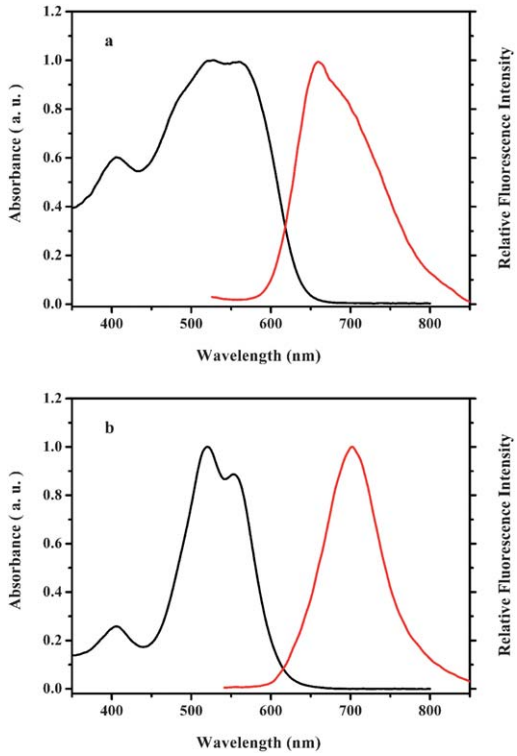

Fig. 7 Normalized absorption (black) and emission (red) spectra of the gels of dimer **1** (a, 3.4 mmol L^{-1}) and hexamer **2** (b, 1.1 mmol L^{-1}) in MCH.

The absorption spectra of the gel of hexamer **2** are also identical to that in the MCH solution. The fluorescence spectra of the gel of hexamer **2** present a further red-shift on the maximum emission peak (701 nm) relative to that in MCH solution (668 nm), which can be ascribed to the further intermolecular aggregation of hexamer **2** in gel, which leads to a more compacted arrangement for the PDI units of hexamer **2**.

Morphology of the gels

To get some insight into the structure of the gels, we choose atomic force microscopy (AFM) to investigate the morphology

on nano scale. Fig. 8A shows the morphology of the gel of dimer **1**. Long one-dimensional fibres of dimer **1** with diameters of 10–20 nm and a very large aspect ratio are found. These long fibres self-assemble into bundles of fibres and collocate with high order in a long range without obvious winding. This may be useful in the construction of organic semiconductor devices.

The gel of hexamer **2** presents a clearly different morphology from that of dimer **1**. Rod like aggregates with diameters of about 80 nm and aspect ratio of about 1 : 10 are found in the image. Most interestingly, the sizes of the aggregates in the image are almost the same. Because the intermolecular interactions between the molecules of hexamer **2** are stronger than those of dimer **1**, as revealed by the absorption and emission spectra, therefore, larger molecular aggregates are expected for hexamer **2** than dimer **1**. We suppose that it is the competition among the different driving forces for molecular aggregation that leads to this result. Three kinds of driving forces for the molecular aggregation for both dimer **1** and hexamer **2** are functioning in our system. They are π–π interactions, hydrogen bonding and hydrophobic interactions between long alkyl chains. It is the hydrophobic interaction between the long alkyl chains that is expected to dominate the intermolecular aggregation process.[11] In dimer **1**, due to the folded conformation of the molecule, the alkyl chains are actually connected at one end of the molecule. In order to achieve the best overlap between the hydrophobic alkyl chains, the phenyl ring must from a face-to-face stacked conformation. Due to the non-coplanar conformation between the PDI ring and the phenyl ring, Fig. 9a, the face-to-face stacking of the phenyl ring will disrupt the face-to-face stacking of the PDI rings. Because the hydrophobic interaction between the alkyl chains dominates the aggregation process, therefore, the π–π stacking between the adjacent PDI units of different molecules can not achieve a best overlap, and therefore, no long range order of the PDI units in the gel of dimer **1** can be observed in the XRD pattern as discussed below. But in hexamer **2**, the long alkyl chains are connected peripherally around the whole molecule, Fig. 9b. In order to achieve the best overlap between the long alkyl chains of different molecule, the adjacent molecules in the aggregates must stack in the correct face-to-face way, without position displacement along all directions. This kind of stacking will certainly lead to a large steric hindrance between the PDI units in the centre and reduce the stability of the molecular aggregates. This is why the molecular aggregates in the gel of hexamer **2** are smaller than those of dimer **1**. This has also explained the distinctive change in the fluorescence spectra of hexamer **2** with concentration increase in MCH.

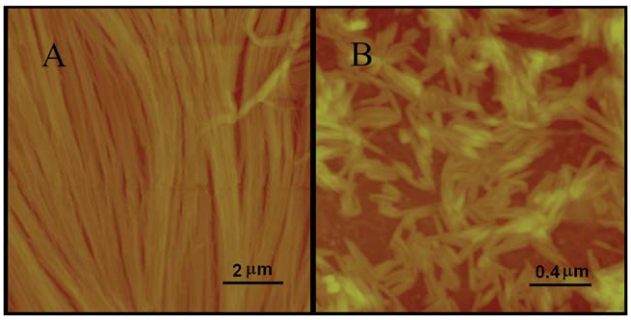

Fig. 8 AFM images of films formed from dropped diluted gel solutions of dimer **1** (A) and (B) hexamer **2** in MCH (1×10^{-4} mol L^{-1}) onto the surface of a SiO_2 substrate and then volatilized slowly in an MCH atmosphere.

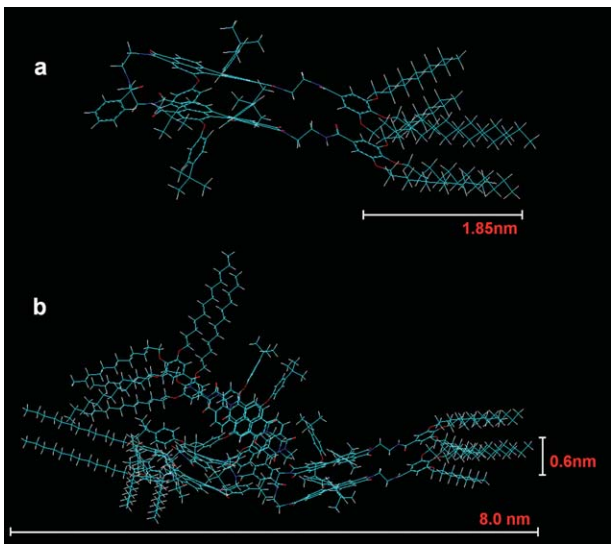

Fig. 9 The energy minimized molecular structure (MM^+) of dimer **1** (a) and hexamer **2** (b).

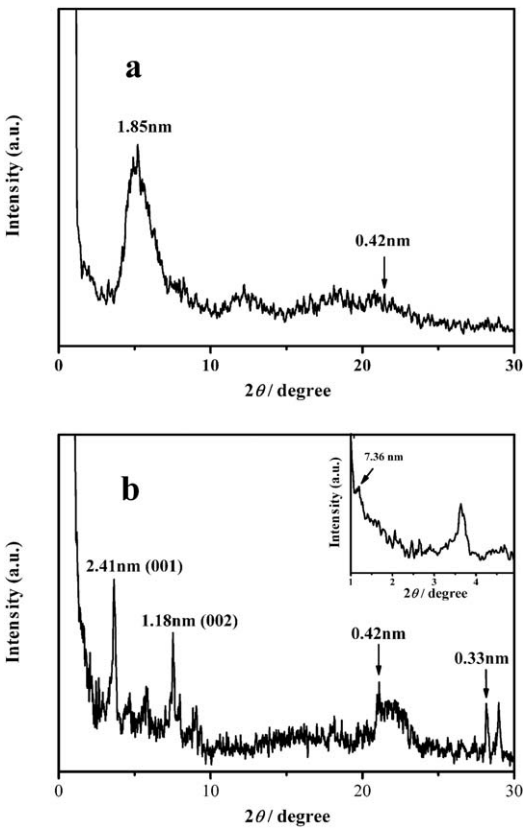

Fig. 10 XRD patterns for dried gels of dimer **1** (a), hexamer **2** (b).

X-Ray diffraction patterns

The internal structure of gels was further investigated by X-ray diffraction (XRD) experiments. Fig. 10 shows the X-ray diffraction patterns of the dried gel of dimer **1** and hexamer **2**. In the X-ray diffraction pattern of dimer **1**, a broad peak in the range of $2\theta = 15$–$25°$, corresponding to a d space of about 0.42 nm, can be assigned to the liquid-like order of the alkyl chains.[32] In the low angle region, two diffraction peaks at $2\theta = 4.8°$ ($d = 1.85$ nm) and 11.6° ($d = 0.76$ nm) are observed. The d space of 1.85 nm is roughly equal to the length of the hydrophobic alkyl chains plus the phenyl ring (1.9 nm) as indicated in Fig. 9a. No diffraction peak at about $2\theta = 29°$, where the diffraction of π–π stacking of aromatic rings normally appears, is observed, which suggests that the PDI units in the gel of dimer **1** do not pack with long range order. This is in accordance with the morphology observation as mentioned above.

The XRD pattern of hexamer **2** shows two reflections in the wide angle region. The broad peak with a d space of 0.42 nm can be assigned to the liquid-like order of the peripheral long alkyl tails, while the other one with a d space of 0.33 nm can be assigned to the stacking distance of PDI cores.[33] In the low angle region, a small diffraction peak at $2\theta = 1.2°$ ($d = 7.36$ nm) may be ascribed to the diameter of the disk like molecule of hexamer **2**. But the d value is little bit smaller than the calculated diameter (8.0 nm, Fig. 9b) based on an energy minimized molecular structure (MM^+), which maybe attributed to chain interdigitation between the adjacent molecules. The peaks at $2\theta = 3.66°$ ($d = 2.41$ nm) and 7.52° ($d = 1.18$ nm) can be assigned to the 001 and 002 diffractions respectively along the vertical direction of the molecular plane, which reveals a high molecular order along this direction in the gel. The calculated thickness of one molecule of hexamer **2** is about 0.6 nm, therefore, one unite cell contains roughly four molecules of hexamer **2**.

Based on the results of the XRD, spectroscopic experiments and morphology examination, we can draw a speculated microstructure for the molecular aggregates of dimer **1** and hexamer **2** in gel respectively. Dimer **1** forms an extend conformation in chloroform with no interactions between the two PDI units. But in MCH, driven by the π–π interaction, hydrogen bonding, and hydrophobic interaction between long alkyl chains, the molecules of dimer **1** change into a folded conformation with the PDI units stacked in a face-to-face way. Along with concentration increase, the folded molecules of dimer **1** further self-assembled into linear fibres driven dominantly by the hydrophobic interaction between the alkyl chains. The thin linear fibres form large aggregates by fibre interlacing and finally give the bundle like morphology with long range order.

For the hexamer **2**, the PDI units in it have similar conformations to that of dimer **1** in MCH. The strong interactions between the long alkyl chains of different molecules drive the molecules of hexamer **2** to stack along the perpendicular direction of the molecular plane into large aggregates. The aggregation process and related diameters for dimer **1** and hexamer **2** are show in Fig. 11.

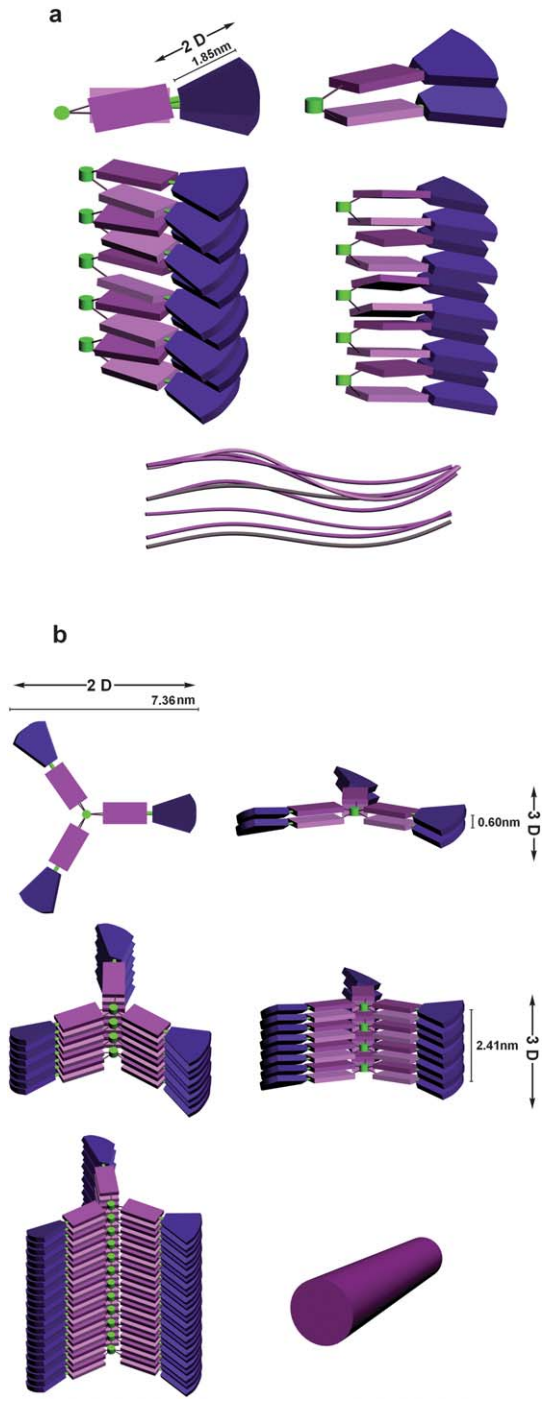

Fig. 11 Proposed aggregation modes of dimer **1** (a) and hexamer **2** (b) in gel on the basis of spectroscopic and XRD analysis.

Conclusions

Two new compounds, dimer **1** and hexmer **2** containing two or six PDI units respectively, are prepared. Due to the presence of efficient π–π interactions, the hydrophobic interactions of the long alkyl chains, and hydrogen bonding, the PDI units in these two compounds try to form face-to-face stacked aggregates even in dilute solution. The PDI units in dimer **1** formed face-to-face stacked structure *via* an intramolecular process. This folded molecule of dimer **1** can form large molecular aggregates in concentrated solution driven by the hydrophobic interactions between the alkyl chains. The PDI units of hexamer **2** form

face-to-face stacked aggregates too, this aggregation is an intramolecular process, but it is seriously affected by the intermolecular aggregation. The peripherally connected long alkyl chains in hexamer **2** have enhanced significantly the hydrophobic interactions between adjacent molecules, but they also disrupt the π–π interaction. This competition between different driving forces for the molecular aggregation of hexamer **2** hinders it from forming large molecular aggregates. This finding revealed that it is possible to control the morphology and size of molecular aggregates by programming the competition between different weak intermolecular interactions.

Experimental

General method

^{1}H NMR spectra were recorded at 300 MHz with the solvent peak as the internal standard (in $CDCl_3$). Electronic absorption spectra were recorded on a Hitachi 4100 spectrometer. Fluorescence spectra were measured on an ISS K2 system. Fluorescence quantum yields were calculated with *N*,*N*′-dicyclohexyl-1,7-di(*p*-*t*-butyl-phenoxyl)-3,4,9,10-tetracarboxylic diimide (Φ_f = 100%) as the standard, all samples were excited at 478 nm. MALDI-TOF mass spectra were obtained on Bruker BIFLEX III mass spectrometer with acyano-4-hydroxycinnamic acid as matrix. The morphology of the dried gel on Si was studied in air by use of a Veeco multimode atomic force microscope (AFM) in tapping mode. The low-angle X-ray diffraction (LAXD) experiment was carried out on a Rigaku D/max-γB X-ray diffractometer.

Materials and methods

All solvents were of analytical grade and purified by using standard methods.[34] 1,7-Di(*p*-*t*-butyl-phenoxyl)-3,4,9,10-tetracarboxylic dianhydried[35] and *N*-(2-aminoethyl)-3,4,5-tris(dodecyloxy)benzamide[30] were synthesized by the procedures described previously.

Preparation compound 4

To a mixture of 1,7-di(*p*-*t*-butyl-phenoxyl)-3,4,9,10-tetracarboxylic dianhydried (344 mg, 0.5 mmol) in 30 mL dried pyridine, a solution of *N*-(2-aminoethyl)-3,4,5-tris(dodecyloxy) benzamide (165 mg, 0.23 mmol) in 10 mL dried pyridine was added dropwise. The mixture was refluxed at 115 °C for 1.5 h. After cooling to room temperature, the solvent was evaporated. The residue was purified by column chromatography on silica gel (CH_2Cl_2 as eluent) to give compound **4**. (32.5 mg, 10%) ^{1}H NMR (300 MHz, $CDCl_3$): δ = 9.65 (m, 2H), 8.59 (m, 2H), 8.35 (d, 2H), 7.50–7.53 (d, 4H), 7.13 (d, 4H), 6.89 (s, 2H), 6.75 (t, 1H), 4.45 (t, 2H), 3.91 (t, 6H), 3.78 (br, 2H), 1.8–1.2 (m, 78H), 0.87 (m, 9H). MS (MALDI-TOF): *m*/*z*, calculated for $C_{89}H_{114}N_2O_{11}$: 1387.91, found 1387.67 [M^+]; Elemental analysis (%) calculated for $C_{89}H_{114}N_2O_{11}$: C 77.02, H 8.28, N 2.02; found: C 77.05, H 8.46, N 2.12.

Preparation compound 3

A mixture of compound **4** (277.5 mg, 0.2 mmol) and imidazole (1.0 g, 14.68 mmol) in dried toluene (25 mL) was refluxed under N_2 for 10 min. Diethylene triamine (10 mg, 0.1 mmol) were added dropwise to the reaction mixture. After reacting for another 0.5 h at this temperature, the solvent was evaporated under reduced pressure and the residue was dissolved in chloroform and washed with water to remove imidazole. The chloroform was removed and the residue was purified by column chromatography on silica gel (methanol/chloroform = 5 : 95, v/v as eluent) to give compound **3** (247.3 mg, 87%). ^{1}H NMR (300 MHz, $CDCl_3$): δ = 9.28 (d, 2H), 9.15 (d, 2H), 8.19 (d, 2H), 8.10 (m, 4H), 8.01 (s, 2H), 7.50 (d, 8H), 7.10 (d, 8H), 7.03 (t, 2H), 6.99 (s, 4H), 4.45 (t, 4H), 4.18 (t, 4H), 3.91 (t, 12H), 3.87 (s, 1H), 3.78 (br, 4H), 2.33–2.35 (t, 4H), 1.8–1.2 (m, 156H), 0.87 (m, 18H). MS (MALDI-TOF): *m*/*z*, calculated for $C_{182}H_{237}N_7O_{20}$: 2842.96, found 2843.88 [M^+]; Elemental analysis (%) calculated for $C_{182}H_{237}N_7O_{20}$: C 76.89, H 8.40, N 3.45; found: C 76.65, H 8.26, N 3.42.

Preparation of hexamer 2

To a mixture of compound **3** (376 mg, 0.15 mmol) and 20 mL CH_2Cl_2, trimesoyl chloride was added dropwise with continuous stirring at room temperature. The resulting mixture was stirred continually at room temperature under a nitrogen atmosphere overnight. After the solvent was evaporated, the residue was purified by column chromatography on silica gel (CH_2Cl_2 as eluent) to give hexamer **2**. In the ^{1}H NMR spectrum of compound **2** in $CDCl_3$ (c = 10^{-4} M), very broad peaks were observed, suggesting the formation of molecular aggregates.[36] ^{1}H NMR (300 MHz, $CDCl_3$): δ = 9.28 (s, broad, 12H), 8.35 (s, broad, 12H), 8.11 (s, broad, 12H), 7.44 (m, 24H), 7.04 (s, 3H), 7.00 (m, 24H), 6.99 (s, 12H), 6.85 (d, 6H), 4.3–4.45 (s, broad, 24H), 3.95 (t, 36H), 3.48–3.85 (broad, 24H), 1.8–1.2 (m, broad, 468H), 0.87 (broad, 54H). MS (MALDI-TOF): *m*/*z*, calculated for $C_{555}H_{711}N_{21}O_{63}$: 8684.96, found 8686.10 [M^+]; Elemental analysis (%) calculated for $C_{555}H_{711}N_{21}O_{63}$: C 76.76, H 88.25, N 3.39; found: C 76.85, H 88.28, N 3.27.

Preparation of dimer 1

To a mixture of compound **3** (142 mg, 0.05 mmol) and 20 mL CH_2Cl_2 benzoyl chloride (7 mg, 0.05 mmol) was added dropwise with continuous stirring at room temperature. The resulted mixture was stirred continually at room temperature under a nitrogen atmosphere overnight. After the solvent was evaporated, the residue was purified by column chromatography on silica gel (CH_2Cl_2 as eluent) to give dimer **1**. ^{1}H NMR (300 MHz, $CDCl_3$): δ = 9.45 (m, 4H), 8.42 (m, 4H), 8.27 (d, 4H), 7.50 (d, 8H), 7.10 (d, 8H), 7.06 (m, 5H), 6.99 (s, 4H), 6.93 (t, 2H), 4.45 (t, 4H), 4.12–4.23 (d, 4H), 3.91 (t, 12H), 3.78 (br, 4H), 1.8–1.2 (m, 160H), 0.87 (m, 18H). MS (MALDI-TOF): *m*/*z*, calculated for $C_{189}H_{241}N_7O_{21}$: 2947.06, found 2948.38 [M^+]; Elemental analysis (%) calculated for $C_{189}H_{241}N_7O_{21}$: C 77.03, H 8.24, N 3.33; found: C 77.25, H 8.32, N 3.12.

Acknowledgements

Financial support from the Natural Science Foundation of China (21073112, 20871055), the Natural Science Foundation of Shandong Province (ZR2010EZ007), the Key lab of photochemistry of Chinese Academy of Science, the Ministry of

Education, and the Graduate Independent Innovation Foundation of Shandong University, are gratefully acknowledged.

Notes and references

1 P. Terech and R. G. Weiss, *Chem. Rev.*, 1997, **97**, 3133–3159.
2 J. H. van Esch and B. L. Feringa, *Angew. Chem., Int. Ed.*, 2000, **39**, 2263–2266.
3 O. Gronwald and S. Shinkai, *Chem.–Eur. J.*, 2001, **7**, 4328–4334.
4 J. B. Beck and S. J. Rowan, *J. Am. Chem. Soc.*, 2003, **125**, 13922–13923.
5 A. M. Shipway, E. Katz and I. Willner, *ChemPhysChem*, 2000, **1**, 18–52.
6 Y. K. Ghosh and S. Bhattacharya, *Chem. Commun.*, 2001, 185–186.
7 S. Murdan, G. Gregoriadis and A. T. Florence, *Eur. J. Pharm. Sci.*, 1999, **8**, 177–185.
8 R. I. Petrova and J. A. Swift, *J. Am. Chem. Soc.*, 2004, **126**, 1168–1173.
9 M. A. Wahab, H. Hussain and C. He, *Langmuir*, 2009, **25**, 4743–4750.
10 X. Zhang, Z. Chen and F. Würthner, *J. Am. Chem. Soc.*, 2007, **129**, 4886–4887.
11 L. Xue, Y. Wang, Y. Chen and X. Li, *J. Colloid Interface Sci.*, 2010, **350**, 523–529.
12 X.-Q. Li, V. Stepanenko, Z. Chen, P. Prins, L. D. A. Siebbeles and F. Würthner, *Chem. Commun.*, 2006, 3871–3873.
13 S. Ghosh, X.-Q. Li, V. Stepanenko and F. Würthner, *Chem.–Eur. J.*, 2008, **14**, 11343–11357.
14 K. Sugiyasu, N. Fujita and S. Shinkai, *Angew. Chem., Int. Ed.*, 2004, **43**, 1229–1229.
15 F. Würthner, B. Hanke, M. Lysetska, G. Lambright and G. S. Harms, *Org. Lett.*, 2005, **7**, 967–970.
16 E. Krieg, E. Shirman, H. Weissman, E. Shimoni, S. G. Wolf, I. Pinkas and B. Rybtchinski, *J. Am. Chem. Soc.*, 2009, **131**, 14365–14373.
17 van T. Boom, R. T. Hayes, Y. Zhao, P. J. Bushard, E. A. Weiss and M. R. Wasielewski, *J. Am. Chem. Soc.*, 2002, **124**, 9582–9590.
18 X. Li, L. E. Sinks, B. Rybtchinski and M. R. Wasielewski, *J. Am. Chem. Soc.*, 2004, **126**, 10810–10811.
19 J. Feng, B. Liang and X. Li, *Langmuir*, 2008, **24**, 11209–11215.
20 Z. Chen, U. Baumeister, C. Tschierske and F. Würthner, *Chem.–Eur. J.*, 2007, **13**, 450–465.
21 Y. Che, A. Datar, K. Balakrishnan and L. Zang, *J. Am. Chem. Soc.*, 2007, **129**, 7234–7235.
22 P. M. Kazmaier and R. Hoffmann, *J. Am. Chem. Soc.*, 1994, **116**, 9684–9691.
23 J. M. Giaimo, J. V. Lockard, L. E. Sinks, A. M. Scott, T. M. Wilson and M. R. Wasielewski, *J. Phys. Chem. A*, 2008, **112**, 2322–2330.
24 W. Wang, L.-S. Li, G. Helms, H.-H. Zhou and A. D. Q. Li, *J. Am. Chem. Soc.*, 2003, **125**, 1120–1121.
25 K. Balakrishnan, A. Datar, R. Oitker, H. Chen, J. Zuo and L. Zang, *J. Am. Chem. Soc.*, 2005, **127**, 10496–10497.
26 K. Balakrishnan, A. Datar, T. Naddo, J. Huang, R. Oitker, M. Yen, J. Zhao and L. Zang, *J. Am. Chem. Soc.*, 2006, **128**, 7390–7398.
27 Y. Chen, L. Chen, G. Qi, H. Wu, Y. Zhang, L. Xue, P. Zhu, P. Ma and X. Li, *Langmuir*, 2010, **26**, 12473–12478.
28 Y. Wang, Y. Chen, R. Li, S. Wang, W. Su, P. Ma, M. R. Wasielewski, X. Li and J. Jiang, *Langmuir*, 2007, **23**, 5836–5842.
29 M. J. Ahrens, L. E. Sinks, B. Rybtchinski, W. Liu, B. A. Jones, J. M. Giaimo, A. V. Gusev, A. J. Goshe, D. M. Tiede and M. R. Wasielewski, *J. Am. Chem. Soc.*, 2004, **126**, 8284–8294.
30 X.-Q. Li, X. Zhang, S. Ghosh and F. Würthner, *Chem.–Eur. J.*, 2008, **14**, 8074–8078.
31 A. Ajayaghosh and S. J. George, *J. Am. Chem. Soc.*, 2001, **123**, 5148–5149.
32 Z. Chen, V. Stepanenko, V. Dehm, P. Prins, L. D. A. Siebbeles, J. Seibt, P. Marquetand, V. Engel and F. Würthner, *Chem.–Eur. J.*, 2007, **13**, 436–449.
33 C. V. Yelamaggad, A. S. Achalkumar, D. S. S. Rao and S. K. Prasad, *J. Org. Chem.*, 2007, **72**, 8308–8318.
34 D. D. Perrin, W. L. F. Armarego, D. R. Perrin, *Purification of Laboratory Chemicals*, Pergamon, Oxford, 1980.
35 A. S. Lukas, Y. Zhao, S. E. Miller and M. R. Wasielewski, *J. Phys. Chem. B*, 2002, **106**, 1299–1306.
36 R. van Hameren, P. Schön, A. M. Buul, J. Hoogboom, Sergiy V. Lazarenko, J. W. Gerritsen, H. Engelkamp, P. C. M. Christianen, H. A. Heus, J. C. Maan, T. Rasing, S. Speller, A. E. Rowan, J. A. A. W. Elemans and R. J. M. Nolte, *Science*, 2006, **314**, 1433–1436.